Modelling a dam break flow in a moving reference frame

Min Gao*, Scott Draper, Lifen Chen, Hugh Wolgamot, Liang Cheng
Oceans Graduate School, The University Western Australia, Perth, WA 6009, Australia.
*Email: min.gao@research.uwa.edu.au

1 INTRODUCTION

Wave overtopping onto the deck of a vessel during severe sea conditions may cause significant damage to topside structures and/or even result in ship loss. Methods for more reliable prediction of green water loads on topside structures therefore remains a key priority for industry.

Over the last 2-3 decades a significant body of research has investigated green water loading on different types of structures placed at different locations on the deck. In some of these studies, the vessel has been held fixed for simplicity. However, it has been shown that vessel motion can influence green water loads. For example, Buchner (1995) emphasized the important role of the vertical velocity of the deck on the pressure on the deck, whilst Zhu et al., (2009) analysed green water on both fixed and oscillating vessels (free in heave and pitch), and stated that the ship motion must be taken into account otherwise the green water loads would be underestimated.

These earlier works showed that vessel motion could influence green water in different ways. Motions affect (i) the general wave-structure interaction and the amount of fluid that enters onto the deck and (ii) the flow behaviours of the on-deck water. In screening of sea-states for green water loads it is straightforward to account for the effect of motions on freeboard exceedance, which is essentially (i), but there is little account taken of (ii). This latter effect could impact the accuracy of screening; events with similar freeboard exceedance but different vessel motion may result in significantly different loads.

In terms of understanding the effect of vessel motion on green water flow on deck, it is not immediately obvious if vessel motions will generally increase or decrease green water loads for the same freeboard exceedance. This is because local (upwards) accelerations of the deck are expected to increase green water flow velocity. However, these accelerations will be maximum when the vessel is displaced downwards in heave and pitch, at which point the upward slope of the pitched deck will act to slow green water. To explore this trade-off further, the present study investigates dam break flows in a moving reference frame that undergoes vessel-like motions (specifically heave and/or pitch motions). Whilst a dam break is not a perfect analogy for green water flow, many researchers have noted and demonstrated the similarities between shipped water and dam break flow (e.g. Buchner, 1995). More advanced modelling approaches could be used to explore the effect of vessel motion on green water (e.g. Greco and Lugni, 2012), but the simple dam break analogy shown in Fig. 1 is an efficient way to explore the problem.

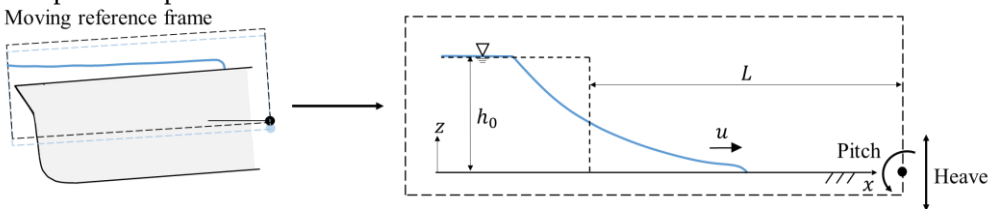

Fig. 1 Sketch of simplification of current problem.

2 PROBLEM DEFINITION AND SOLUTION

As in the classical dam break model, in this work a dam is defined in terms of its initial height h_0 located within a moving reference frame (Fig. 1). Heave displacement and pitch rotation of the reference frame containing the dam break are modelled as sinusoidal functions of time with period T_h and T_p, and amplitudes $a_h(T_h/2\pi)^2$ and $\alpha_p(T_p/2\pi)^2$, respectively. Here, a_h and α_p are the peak heave acceleration and pitch rotational acceleration, respectively. Phases of the motions ϕ_h and ϕ_p are defined relative to the time of the initial dam break. The last parameter needed to define the problem is the distance between the initial dam location and the point about which the reference frame rotates, denoted by L. Combining these parameters with the acceleration due to gravity g, leads to several non-dimensional parameters, including the normalized accelerations (a_h/g, $a_p/g = \alpha_p L/g$), periods ($T_h/(h_0/g)^{1/2}, T_p/(h_0/g)^{1/2}$) and radius of rotation L/h_0 in addition to the relative phase of the motions.

To determine practical ranges for these non-dimensional parameters a seakeeping analysis for a Floating, Production, Storage and Offloading (FPSO) unit located on the North West Shelf of Australia has been

undertaken (using the same model and sea states as those adopted in Chen et al., 2019) The results of this analysis show that in events leading to freeboard exceedance, the vertical motion at the bow due to pitch was around three times that due to heave. Taking the peak wave period to be equal to the periods of motion T_h and T_p, and the maximum freeboard exceedance to be the initial dam height h_0, the analysis indicates the following ranges: a_h/g =0.04~0.08, a_p/g =0.14~0.24, $T_h/(h_0/g)^{1/2}$ =12.5~28.2, and $T_p/(h_0/g)^{1/2}$ =15.5~28.2. With respect to ϕ_h and ϕ_p, the vessel heave and pitch at the time of maximum freeboard exceedance showed some variation, but were often associated with the time of minimum heave and pitch (resulting in negative freeboard/vertical motion); hence these can be assumed to take values that ensure minimum pitch and heave when the dam breaks. The normalised radius L/h_0 of the pitch had a mean value of about 40.

Over this non-dimensional parameter-space the dam break problem has been simulated using both CFD and the Shallow Water Equations (SWEs). In the CFD simulations, the Navier-stokes equations are solved using the *interDyMFoam* provided by an open source CFD package OpenFOAM to describe the flow motion in a moving frame. The computational domain is forced to heave and pitch with a prescribed motion and the Volume of Fluid method is used to track the free surface. In the SWE simulations, the 1D shallow water equations (Eq. 1) have been solved using the Harten Lax van Leer Riemann solver (Harten et al., 1983)

$$\frac{\partial h}{\partial t}+\frac{\partial hu}{\partial x}=0, \qquad \frac{\partial uh}{\partial t}+\frac{\partial u^2 h}{\partial x}=-0.5\frac{\partial(a_z h^2)}{\partial x}+a_x h, \tag{1}$$

where u represents the depth-averaged horizontal velocity, h is the water depth and both a_z and a_x represent additional accelerations introduced by the vessel motion, including the Coriolis, centripetal and Euler components. These terms are modelled following the approach derived in Huang and Hsiung (1996).

3 SIMULATION RESULTS

Fig. 2a presents free surface profiles obtained from CFD simulations of dam break events in a fixed reference frame, and an oscillating reference frame representing relatively large vessel motion (parameters are given in caption). Results are plotted at three typical instants : $1.1(h_0/g)^{1/2}=0.05T_h=0.05T_p$, $4.39(h_0/g)^{1/2}=0.2T_h$ and $10.96(h_0/g)^{1/2}=0.5T_h$. It can be seen that the motion does not drastically alter the flow profile but does result in noticeable changes. For instance, for the moving dam break the water surface elevation reduces faster upstream of the dam (x <0) owing to the downward pitch of the vessel, whilst the upstream profile still maintains a similar run-out speed due to the increased acceleration due to motion. To investigate these changes in surface profile in more detail, Fig. 2b plots the horizontal momentum flux for both dam break scenarios. This momentum flux has been calculated using a set of numerical gauges orientated normal to the bed and spaced $0.1h_0$ apart. It can be seen that the momentum flux for the moving dam break is different from the fixed case; at the first time instant the momentum flux is larger due to motion, whilst it is lower at the two later times. Noting that the Froude number of the flow on deck is large, the horizontal momentum flux should correlate well with the load on large structures capable of completely deflecting the flow, implying that the motion is increasing the damage potential of the dam break flow in this example.

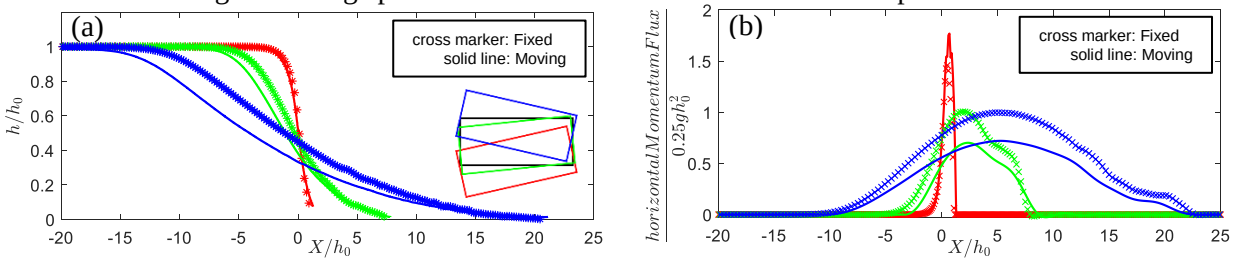

Fig. 2 Free surface profile (a) and horizontal momentum flux (b) at three instants in time (cross-referenced in Fig. 3) obtained from CFD for a fixed and representative moving reference frame with (a_h/g =0.08, a_p/g =0.24, and $T_p/\sqrt{h_0/g}=T_h/\sqrt{h_0/g}$= 21.9). Phases chosen to ensure minimum pitch and heave when the dam breaks. L/h_0 =40. A cartoon on lower left of Fig.(a) shows the position of the moving frame at three time instants and the fixed frame(black).

3.1 The evolution of momentum flux in time

A number of characteristics associated with green water flow influence load. In this abstract, we focus on momentum flux which, as noted above, is likely to be a good indication of the load on large structures. In more general scenarios, both the depth and the velocity of the flow can also be important for predicting loads. We define the maximum horizontal momentum flux in space at any time instant as the Maximum Momentum Flux (MMF). For reference, the MMF of a fixed dam break flow on a flat bed modelled using the SWEs is $0.25gh_0^2$ and is constant in time (e.g. Chanson, 2006).

The evolution of MMF calculated using CFD and the SWE solver for a heaving, pitching and combined heaving and pitching dam break is shown in Fig. 3. The MMF of a classical dam break in a fixed reference frame is also presented as a reference to distinguish the effect of vessel motion. The three example cases shown have the largest normalised acceleration across the practical ranges described in Section 2, hence they display the most evident effects of vessel motion on MMF. It can be seen that as the dam initially breaks, the MMF increases to a peak value, followed by a drop which is similar to that observed for the fixed dam break. Following this, the MMF oscillates in time owing to the heave and pitch motions which result in varying acceleration and bed slope, whilst for the fixed dam break the MMF becomes constant in time and close to the analytical estimate of $0.25gh_0^2$. Based on these observations, two typical stages in the dam break flow are identified: (i) the initial stage where the CFD result has a sharp increase in MMF followed by a rapid descent; and (ii) the later stage where the MMF fluctuates and the results from CFD and SWE agree with each other well. Across the range of parameters considered in this study, the duration of the initial stage did not vary significantly, lasting approximately $(2.7\sim3.1)(h_0/g)^{1/2}$.

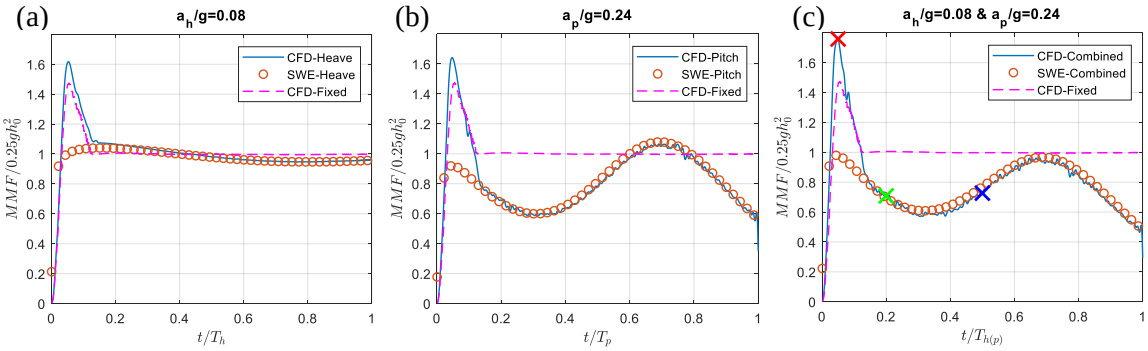

Fig. 3 Evolution of MMF for (a) heave ($a_h/g = 0.08$, $T_h/\sqrt{h_0/g}$= 21.9), (b) pitch ($a_p/g = 0.24$, $T_h/\sqrt{h_0/g}$= 21.9) and (c) combined heave and pitch with (a_h/g =0.08, a_p/g =0.24, and $T_p/\sqrt{h_0/g} = T_h/\sqrt{h_0/g}$= 21.9). Crosses indicate the time instants in Fig. 2

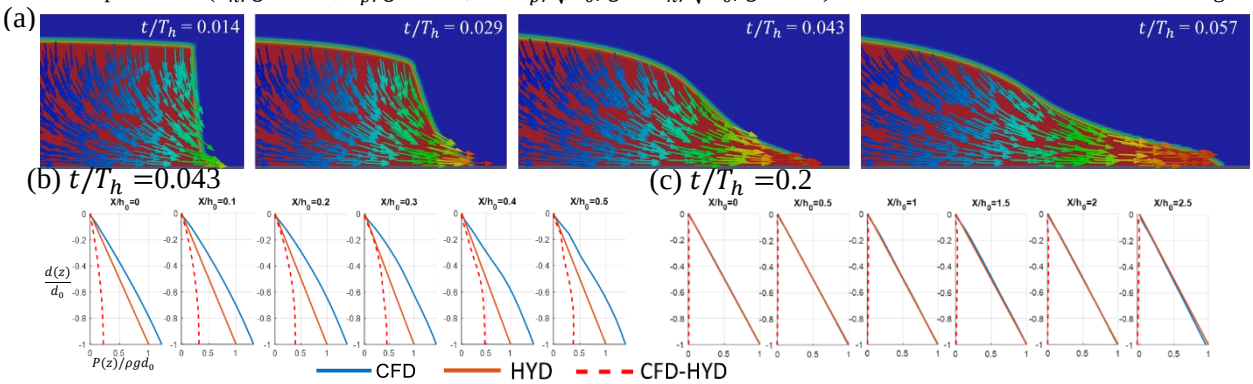

Fig. 4 (a) Velocity vectors at different times for a heaving dam break ($a_h/g = 0.08$, $T_h/\sqrt{h_0/g}$= 21.9). Pressure distribution with depth in (b) the initial stage (t/T_H = 0.043) and (c) the later stage (t/T_H = 0.2) at six locations for the same heave case. d_0 represents water depth on bed at that location, whilst $d(z)$ and $P(z)$ represent depth and pressure through the water column. The pressure obtained from CFD is referred as "CFD", and hydrostatic pressure is referred to as "HYD".

The results in Fig.3 are consistent with the experimental and numerical study by Stansby et al. (1998), which indicated that the analytical solution of SWEs agrees with the experimental measument only after a bore is established. The velocity vectors from CFD at a few instants in time are shown in Fig. 4a for a heaving dam break just after release. It can be seen that the vertical flow funnels into a horizontal jet which results in an increase in MMF during the initial stage of the dam break. This funnelling is associated with a non-hydrostatic pressure distribution with depth (Fig. 4b), explaining the lack of agreement with the SWEs during the initial stage. In contrast, at later times (Fig. 4c), the pressure distribution with depth becomes hydrostatic satisfying the shallow water assumption. The results from CFD and the SWEs agree well with each other at this time.

3.2 Peak MMF

The peak MMF in time provides an upper bound estimate of damage potential. This peak is plotted in Fig. 5 for heaving cases (left), pitching cases (middle) and combined heaving and pitching cases (right) for a range of normalised acceleration and period. In each plot the peak MMF has been normalized by the peak MMF of the classical dam break calculated using CFD and the phase of the motions is chosen to ensure minimum heave and pitch when the dam breaks. The assumption T_p=T_h and a_p=3a_h is used in the combined case, as suggested by the seakeeping analysis mentioned in Section 2. Focusing first on heave, it can be seen that heave motion always results in an increase in peak MMF. This increase is almost linear with normalised acceleration (hence

it essentially increases local gravity) and is not sensitive to normalised period over the range of parameters considered because it happens during the initial stage of the dam break. For pitch the same is not true; for sufficiently large normalised period the peak MMF reduces to values close to and below that for a fixed dam break. This is because for these cases the pitch angle (shown using contour lines in Fig. 5) increases when the dam break occurs, which acts to reduce the MMF. Nevertheless, for the vast majority of the parameter space the peak MMF is increased, indicating that acceleration effects are more important than slope effects for most practical scenarios. Comparing the heave and pitch only cases, it is clear that that increase in peak MMF is bigger in the latter case. This is not unexpected given that the range of normalised pitch accelerations (chosen based on the seakeeping analysis) are larger than those due to heave, emphasising the relative importance of pitch motion. Finally, in the combined heave and pitch scenarios, the heave acceleration effectively adds to the acceleration induced by pitch. This results in a further increase in peak MMF up to values of close to 20% over the range of parameters considered.

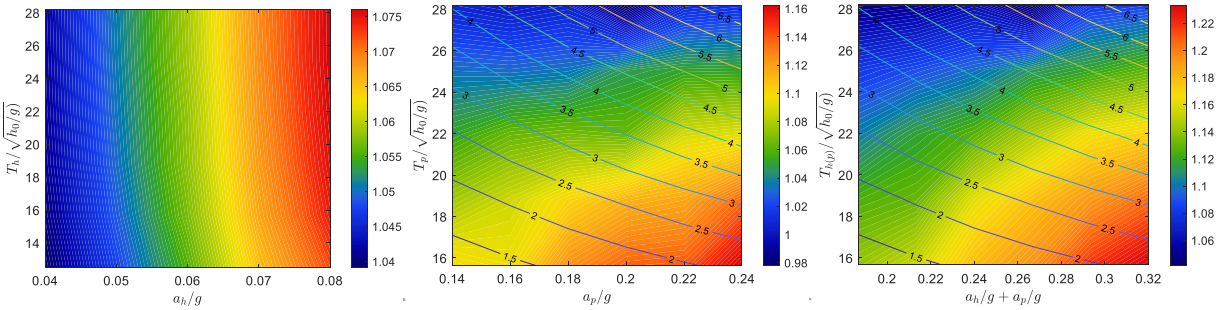

Fig. 5 Peak MMF of heave(left), pitch(middle) and combined(right) case obtained from CFD. The contour line with number is the angle of pitch motion in degree.

4 CONCLUSIONS

The dam break flow in a moving reference frame is numerically studied as an approximation of green water flow on a moving deck. As for fixed dam break flow, two stages in the evolution of the dam break are identified; the initial non-hydrostatic stage that has a sharp increase in horizontal MMF followed by a rapid descent, and the later hydrostatic stage where the MMF oscillates in time. In the initial stage, the MMF reaches its largest value. This peak may be higher or lower than that observed in a classic (fixed) dam break flow, but over the majority of the parameter space believed to be relevant to ship motions, heave and pitch lead to increases in peak MMF. These increases are typically on the order of 5-20%, hence they are not insignificant but at a level where fixed models are still likely to provide useful insight into green water loading. For times that do not coincide with peak MMF, motion can lead to an increase or decrease in MMF compared to a fixed dam break depending on the phase of the deck oscillation.

During the workshop these findings will be compared to experimental data for a simplified FPSO geometry (similar to that modelled in Chen et al. 2021), recently tested at 1:64 scale in the large wave basin at Shanghai Jiao Tong University. Simultaneous measurements of vessel motion, relative wave elevation and load on a topside structure placed close to the bow, allow inference of the effect of vessel motion on green water load.

ACKNOWLEDGEMENT

This work was supported by the ARC Industrial Transformation Research Hub for Offshore Floating Facilities which is funded by the Australian Research Council, Woodside Energy, Shell, Bureau Veritas and Lloyds Register (Grant no. IH140100012). The support in resources provided by the Pawsey Supercomputing Centre. HW is supported by an Australian Research Council (ARC) Early Career Fellowship (DE200101478).

REFERENCES

Buchner, B. The impact of green water on FPSO design. 1995 Houston, TX, United states. Offshore Technology Conference, 45-57.

Chanson, H. Analytical solutions of laminar and turbulent dam break wave. Proceedings of the International Conference on Fluvial Hydraulics, River Flow, 2006. 465-474.

Chen, L., Taylor, P. H., Draper, S., Wolgamot, H., Milne, I. A. & Whelan, J. R. 2019. Response based design metocean conditions for a permanently moored FPSO during tropical cyclones: Estimation of greenwater risk. *Applied Ocean Research*, 89, 115-127.

Greco, M. & Lugni, C. 2012. 3-D seakeeping analysis with water on deck and slamming. Part 1: Numerical solver. *Journal of Fluids and Structures*, 33, 127-147.

Harten, A., Lax, P. D. & Van Leer, B. 1983. On Upstream Differencing and Godunov-Type Schemes for Hyperbolic Conservation Laws. *SIAM Review*, 25**,** 35-61.

Huang, Z. & Hsiung, C.-C. 1996. Nonlinear Shallow-Water Flow on Deck. Journal of Ship Research, 40, 303-315.

Stansby, P. K., Chegini, A. & Barnes, T. C. D. 1998. The initial stages of dam-break flow. *Journal of Fluid Mechanics*, 374**,** 407-424.

Zhu, R., Miao, G. & Lin, Z. 2009. Numerical Research on FPSOs With Green Water Occurrence. *Journal of Ship Research*, 53**,** 7-18.

Chen, L. F., Taylor, P. H., Ning, D. Z., Cong, P. W., Wolgamot, H., Draper, S. & Cheng, L. 2021. Extreme runup events around a ship-shaped floating production, storage and offloading vessel in transient wave groups. Journal of Fluid Mechanics, 911, A40.